CORE
Metadata, citation and similar papers at core.ac.uk
Provided by NASA Technical Reports Server

NASA/TM-2008-215327

Signal Analysis Algorithms for Optimized Fitting of Nonresonant Laser Induced Thermal Acoustics Damped Sinusoids

R. Jeffrey Balla and Corey A. Miller
Langley Research Center, Hampton, Virginia

July 2008

The NASA STI Program Office . . . in Profile

Since its founding, NASA has been dedicated to the advancement of aeronautics and space science. The NASA Scientific and Technical Information (STI) Program Office plays a key part in helping NASA maintain this important role.

The NASA STI Program Office is operated by Langley Research Center, the lead center for NASA's scientific and technical information. The NASA STI Program Office provides access to the NASA STI Database, the largest collection of aeronautical and space science STI in the world. The Program Office is also NASA's institutional mechanism for disseminating the results of its research and development activities. These results are published by NASA in the NASA STI Report Series, which includes the following report types:

- TECHNICAL PUBLICATION. Reports of completed research or a major significant phase of research that present the results of NASA programs and include extensive data or theoretical analysis. Includes compilations of significant scientific and technical data and information deemed to be of continuing reference value. NASA counterpart of peer-reviewed formal professional papers, but having less stringent limitations on manuscript length and extent of graphic presentations.

- TECHNICAL MEMORANDUM. Scientific and technical findings that are preliminary or of specialized interest, e.g., quick release reports, working papers, and bibliographies that contain minimal annotation. Does not contain extensive analysis.

- CONTRACTOR REPORT. Scientific and technical findings by NASA-sponsored contractors and grantees.

- CONFERENCE PUBLICATION. Collected papers from scientific and technical conferences, symposia, seminars, or other meetings sponsored or co-sponsored by NASA.

- SPECIAL PUBLICATION. Scientific, technical, or historical information from NASA programs, projects, and missions, often concerned with subjects having substantial public interest.

- TECHNICAL TRANSLATION. English-language translations of foreign scientific and technical material pertinent to NASA's mission.

Specialized services that complement the STI Program Office's diverse offerings include creating custom thesauri, building customized databases, organizing and publishing research results ... even providing videos.

For more information about the NASA STI Program Office, see the following:

- Access the NASA STI Program Home Page at ***http://www.sti.nasa.gov***

- E-mail your question via the Internet to help@sti.nasa.gov

- Fax your question to the NASA STI Help Desk at (301) 621-0134

- Phone the NASA STI Help Desk at (301) 621-0390

- Write to:
  NASA STI Help Desk
  NASA Center for AeroSpace Information
  7115 Standard Drive
  Hanover, MD 21076-1320

NASA/TM-2008-215327

Signal Analysis Algorithms for Optimized Fitting of Nonresonant Laser Induced Thermal Acoustics Damped Sinusoids

R. Jeffrey Balla and Corey A. Miller
Langley Research Center, Hampton, Virginia

National Aeronautics and
Space Administration

Langley Research Center
Hampton, Virginia 23681-2199

July 2008

Acknowledgments

The authors acknowledge many helpful discussions with G. E. Plassman.

The use of trademarks or names of manufacturers in this report is for accurate reporting and does not constitute an official endorsement, either expressed or implied, of such products or manufacturers by the National Aeronautics and Space Administration.

Available from:

NASA Center for AeroSpace Information (CASI)
7115 Standard Drive
Hanover, MD 21076-1320
(301) 621-0390

National Technical Information Service (NTIS)
5285 Port Royal Road
Springfield, VA 22161-2171
(703) 605-6000

Signal Analysis Algorithms for Optimized Fitting of Nonresonant Laser Induced Thermal Acoustics Damped Sinusoids

R. Jeffrey Balla and Corey A. Miller
NASA Langley Research Center
Hampton, Va. 23681-2199

Abstract

This study seeks a numerical algorithm which optimizes frequency precision for the damped sinusoids generated by the nonresonant LITA technique. It compares computed frequencies, frequency errors, and fit errors obtained using five primary signal analysis methods. Using variations on different algorithms within each primary method, results from 73 fits are presented. Best results are obtained using an AutoRegressive method. Compared to previous results using Prony's method, single shot waveform frequencies are reduced ~0.4% and frequency errors are reduced by a factor of ~20 at 303K to ~ 0.1%. We explore the advantages of high waveform sample rates and potential for measurements in low density gases.

1. Introduction

Interest in the nonresonant Laser-Induced Thermal Acoustics (LITA) optical diagnostic comes from its capability to make high-accuracy (typically 1%) measurements of temperature[1], sound speed[2], velocity[3], and pressure[4] during a single laser pulse. There are few instrumental methods combining this level of accuracy and temporal resolution. LITA data can be used to advance our understanding in a wide variety of scientific fields.

Our nonresonant LITA apparatus and the theory behind it have been described previously [1]. Briefly, a high-peak-power pulsed (10 ns) laser is split into two beams and crossed at a small angle; typically 1 degree. At the focus, the resulting interference pattern creates two counter propagating acoustic wave packets by electrostriction. As they counter propagate, they interfere constructively and destructively. A second continuous laser beam is Bragg scattered off the acoustic wave packets. This creates an intensity modulation in the scattered laser light at a frequency (~20 MHz) twice that of the counter propagating acoustic waves (~10 MHz). This frequency can be related to sound speed in the gas. Temperature can be calculated if gas composition is known. These ultrasonic acoustic waves rapidly decay by acoustic absorption. Hence signals reflect the intensity modulation of the counter propagating acoustic waves convolved with a damping function created by acoustic absorption. Resulting waveforms resemble damped sinusoids.

2. Previous Analysis Methods

Data and waveforms analyzed in this study were generated previously (1). Unlike reference 1, this study uses raw LITA data not normalized by probe laser temporal variation. This weakly perturbs the waveform shape but has negligible effect on computed frequency. This approach forces the mathematics to be more robust.

In early work on LITA, an analytical expression [4] was derived to describe these waveforms. Simplified, it is essentially a sinewave convolved with a decaying exponential which must be squared to reproduce the waveform. It is given as

$$Y(t) = \{ A * (\exp -k*t) + [B * \cos(\omega* t+ \phi) * (\exp - C* t)] \}^2 \quad (1)$$

where A and B are amplitudes related to the resonant and nonresonant LITA components respectively. k is related to gas properties and grating frequency, ω is the acoustic frequency of interested in this study and related to the sound speed, ϕ is a phase factor, and C is related to acoustic damping. Initial guesses were required and fits were optimized using a Levenberg-Marquardt algorithm.

Equation 1 is applicable to both resonant and nonresonant LITA. In resonant LITA (i.e. A >B), an appropriate molecule such as NO_2 is seeded into the flow and excited to create a strong thermal grating and high signal levels on an essentially flat baseline. In our applications with large-scale wind tunnel applications, seeding is undesirable. It is expensive, potentially toxic, and perturbs the flow. Instead, we pursued nonresonant LITA (i.e. B >A) so the first term in Equation 1 is presumed negligible. Nonresonant LITA creates acoustic waves in any fluid using electrostriction. Unfortunately, nonresonant LITA signals are typically orders-of-magnitude weaker than resonant LITA. Signal to noise (S/N) ratios are reduced. Baselines are nonzero and often time dependent. Pulse-to-pulse spatial nonuniformities in the laser beam can create a waveform where the amplitude of the second peak is larger than the first. All these experimental difficulties combine to produce a unique waveform shape that varies on a pulse to pulse basis. Hence, nonresonant LITA waveforms only approximately resemble damped sinusoids.

A variety of gas parameters can be extracted from nonresonant LITA waveforms. Our thermometry[1], sound speed[2], velocimetry[3], and pressure [4] applications require only waveform frequency. Hence, this study concentrates on minimizing frequency error. Data analyzed here was taken at a fixed gas temperature, pressure, and composition. This fixes the sound speed in the gas.

In Reference 1, we recommended Prony's method. It was developed specifically for fitting damped sinusoids. Unlike Equation 1, it does not require good initial guesses and is computationally faster. Results [1] indicate Equation 1 and Prony's method both produce frequencies with ~1-3% single pulse accuracy and precision for nonresonant LITA waveforms. In terms of frequency error, these are treated as equivalent methods in this study.

3. Results and Discussion

Since Reference 1 was published, new signal analysis methods have become available. This study explores several to find the frequency components in the LITA waveforms and determines which produce the lowest fit and frequency errors. To eliminate extensive programming of complex math routines, we use the AutoSignal (www.systat.com)) software package. It is designed specifically to model damped and undamped sinusoids. We select five main signal analysis methods (Fourier Transform, AutoRegressive, Prony, Minimum Variance, and EigenAnalysis) and test different algorithms associated with each one. The AutoSignal manual contains a discussion of advantages of each method, waveforms to which they are applicable, and literature references for further reading. Decisions for rejecting some algorithms are based on those discussions. AutoSignal abbreviations are adopted here and identified in Table 1.

The errors in this study are based on comparison between experimental and computed waveforms. Best results have errors which are sufficiently low that their accuracy cannot be verified using current LITA instrumentation. We emphasize that this work is a study in computed precision not accuracy.

3.1 Waveform Temporal Optimization

Typical nonresonant LITA waveforms are shown in Figure 1. Initial signal growth is dominated by electrostriction. It would be difficult to model this growth even if data were available. Acoustic decay of the counter propagating acoustic waves dominates near the first peak. After 9-10 cycles, background signal dominates. We expect optimal fit results between these locations. Rather than attempt to model these complex effects, we choose the simpler solution of selecting the intermediate points which produce minimum computed frequency errors.

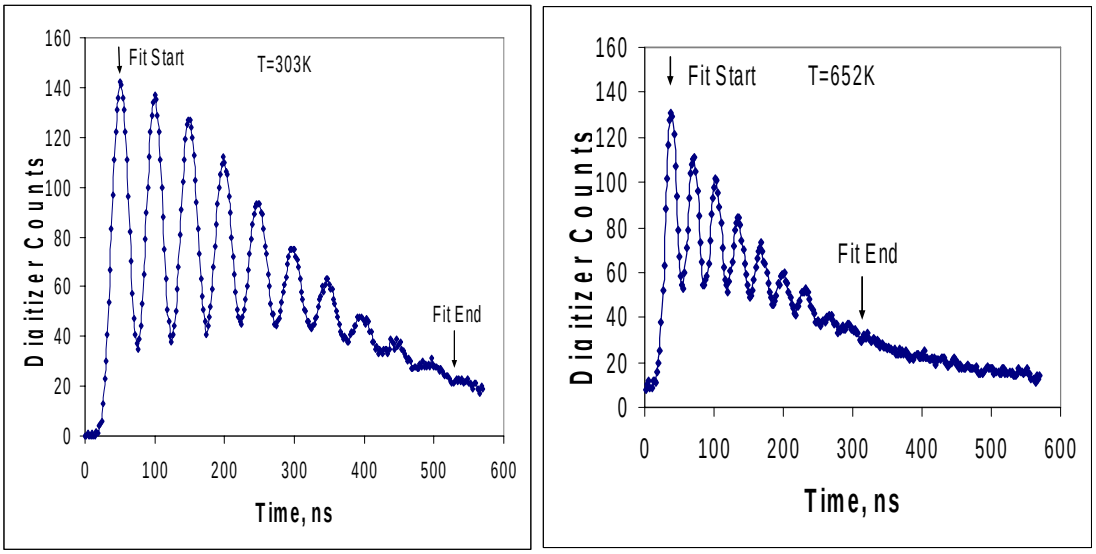

Figure 1. Typical single-laser-pulse damped sinusoidal waveforms produced by nonresonant LITA at 303K and 652K. Data is taken from Reference 1. Waveform contains 25 data points per cycle at 303K, contains 285 total data points, and is uniformly sampled in 2 ns increments.

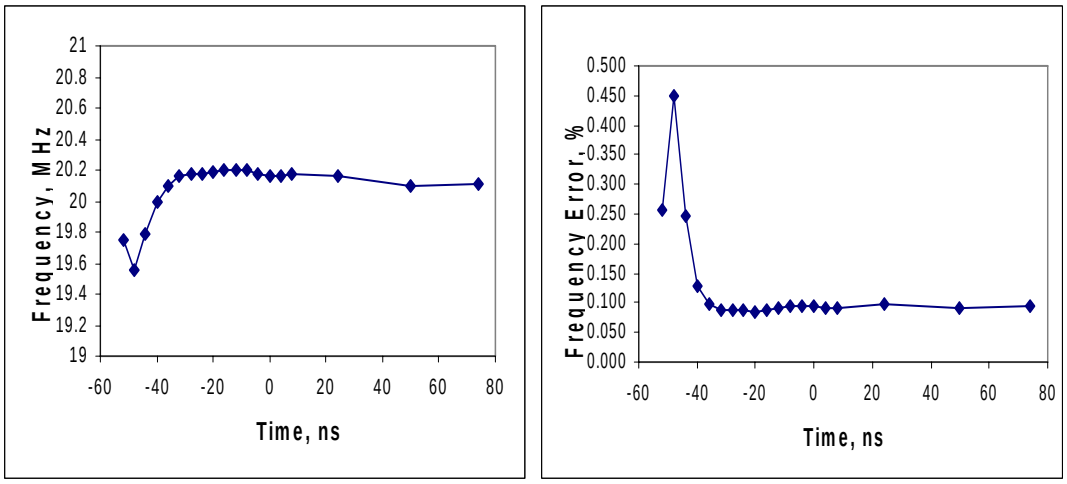

Figure 2. Computed frequency (MHz, left) and frequency error (%, right) (rms frequency error / frequency * 100) as a function of start time for 303 K data in Figure 1 using an AutoRegressive spectrum algorithm (Data Svd FB, order 50, signal subspace 4) and non-linear optimization. First peak in Figure 1 occurs in Figure 2 at t=0 ns. Second peak occurs at t=50 ns.

Computed frequency and frequency error results as we sequentially removed initial points from each waveform in 4 ns steps are shown in Figure 2. Errors are minimal after initial baseline is removed and signals are > 15% of the first peak value. For ease of analysis, we discard all data prior to the top of the first peak in Figure 1. We designate it as t=0 in Figure 2 and fit start in Figure 1. A similar study was performed for the trailing data. They show a very weak minimum for both temperatures near the top of the second to last visible peak. However, frequencies vary < 0.2% and fit uncertainties < 8% as trailing points are removed. For ease of analysis, we discard all data after the second to last visible peak. Resulting fit start and end points are shown in Figure 1. Similar result was found for 652K data in Figure 1.

3.2 Algorithm Comparison

Algorithm comparison using data in Figure 1 at 303 K is shown in Table 1. Using five main signal analysis methods and variations on multiple algorithms within each, we present results from 73 fits. Extracting the frequency of damped sinusoids with high precision and accuracy is an old and unsolved problem in mathematics. Modern publications recognize the **AutoRegressive spectrum method** (hereafter designated **AR**) as the best frequency estimator.

Table 1. Frequencies, Frequency Errors, and Fit Errors Computed using Single Pulse LITA Data in Figure 1 at 303K. Frequency Error (%) = Standard Deviation / Frequency * 100. Dashed Line Indicates no Convergence.

SS = Signal Subspace SVD = Singular Value Decomposition
NE = Normal Equations
F, B, FB = Forward, Backward, Forward and Backward Prediction Algorithm

Fourier Spectrum

Transform	Freq, MHz	Freq Error,%
Best Exact N	20.580	1.66
FFT Radix 2	20.268	1.60
Prime Factor	20.729	1.68
Mixed Radix	20.580	1.66
Chirp-Z	20.580	1.66

AutoRegressive Spectrum – All use SS=4, no non-linear optimization

Algorithm	Order	Freq, MHz	Fit Error,%	
AutoCorr	40	20.639	2.24	
Burg	30	20.023	1.40	
Nrml F	40	20.879	2.15	
Data F	30	20.244	1.50	
Data B	30	20.312	1.78	
Data FB	30	20.306	1.40	
Data SVD F	50	20.091	7.45	
Data SVD B	50	20.176	8.22	
Data SVD FB	30	20.218	3.18	
Data SVD FB	40	20.186	5.35	
Data SVD FB	**50**	**20.177**	**5.26**	**optimal freq. fit**
Data SVD FB	60	20.180	7.89	
Data SVD FB	70	20.171	9.39	
Data SVD FB	80	20.162	9.29	

Non-Linear Optimization - Least Squares Minimization Method

Algorithm	Order	Freq, MHz	Freq. Error, %	
Data SVD FB	40	---------	-----	
Data SVD FB	**50**	**20.169**	**0.096**	**optimal fit**
Data SVD FB	60	20.169	0.096	
Data SVD FB	70	20.169	0.096	
Data SVD FB	80	---------	-----	

Initial Algorithm: Data SVD FB, Order 50, SS=4
Non-Linear Optimization Parameters
Model: Exp. Damped Sine, 2 frequency components, unshared frequency and phase

Minimization Method	Freq. MHz	Freq. Error, %	r^2	
Least Squares	**20.169**	**0.096**	**0.990**	**optimal fit**
Least Abs Dev	20.131	0.11	0.988	
Lorentzian	20.097	0.16	0.973	
Pearson 7	20.153	0.11	0.985	

Prony Spectrum - All use SS=2

Algorithm	Order	Freq, MHz	Freq. Error, %
Damped	10	20.417	2.3
Damped	15	20.252	2.1
Damped	20	20.210	2.3
Damped	**30**	**20.245**	**2.3 – Ref. 1 result**
Damped	40	20.089	3.4
Damped	50	20.259	3.4
Damped SVD	30	17.802	39.5
Damped SVD	40	33.336	60.7
Damped SVD	50	19.799	3.3
Damped SVD	60	20.948	3.4
Damped SVD NE	30	17.964	35.6
Damped SVD NE	40	17.792	12.2

Minimum Variance Spectrum

Algorithm	Order	Freq, MHz	Freq. Error, %
SumArBurg	30	20.020	1.6
SumArBurg	40	19.989	1.6
SumArDataF	30	20.203	1.6
SumArDataF	40	20.203	1.6
SumArDataB	30	20.294	1.6
SumArDataB	40	20.294	1.6
SumArDataFB	30	20.264	1.6
SumArDataFB	40	20.264	1.6
Musicus	30	20.020	1.6
Musicus	40	19.989	1.6
Capon-Kay	30	20.203	1.6
Capon-Kay	40	20.203	1.6

EigenAnalysis Spectrum - All use SS=4

Algorithm	Order	Freq, MHz	Freq. Error, %
MUSIC Fwd	30	20.228	1.6
MUSIC Fwd	40	20.192	1.6
MUSIC Fwd	60	20.161	1.6
MUSIC Fwd	100	20.147	1.6
EigVec Fwd	30	20.229	1.6
EigVec Fwd	40	20.195	1.6
EigVec Fwd	60	20.156	1.6
EigVec Fwd	100	20.066	1.6
MUSIC FB	30	20.211	1.6
MUSIC FB	40	20.200	1.6
MUSIC FB	50	20.179	1.6
MUSIC FB	60	20.161	1.6
MUSIC FB	**80**	**20.171**	**0.32**
MUSIC FB	100	20.152	0.33
EigVec FB	30	20.218	1.6
EigVec FB	40	20.200	1.6
EigVec FB	45	20.186	0.32
EigVec FB	**50**	**20.179**	**0.32**
EigVec FB	60	20.152	0.32
EigVec FB	80	20.173	0.32
EigVec FB	100	20.156	0.32

In the AR method, if a model can be fit to a data stream, it can be transformed into the frequency domain instead of the data upon which it is based. Hence, it produces a continuous and smooth spectrum. In an AR model, a value at time t is based on a linear combination of prior values (Forward prediction), combination of subsequent values (Backward prediction) or both (Forward-Backward prediction). This is a linear model which gives rise to rapid and robust computations. The singular value decomposition (SVD) improves results using in-situ noise filtration.

AR has several algorithm variations including Data, AutoCorr, Burg, and Normal (Nrml). Most can be run using F, B or FB prediction. Each of these can vary order creating a large number of combinations. Discussions of these methods are provided to minimize the number of variations tested.

AutoCorr (sometimes referred to as Yule-Walker method) is common in most statistical packages but has the least frequency resolution. The Burg Algorithm (Max Entropy Method) is most widely known but designed for harmonic detection. The NRML algorithm uses a least-squares normal equations approach. Sums incur loss of precision which can lead to reduced frequency resolution. The DATA algorithm processes the full F, B, or FB prediction data matrix. This approach has no loss of precision but requires extensive computation. It is widely recognized as the most accurate of AR processing procedures. The DATA FB algorithm is also known as the modified covariance method. The DATA SVD FB algorithm is known as the Principal Component AutoRegressive method (PCAR). The SVD procedure uses an eigendecomposition to discard the noise eigenmodes when the AR coefficients are computed. The combination of DATA, SVD, and FB produces an algorithm with extraordinary frequency estimation.

AutoSignal software has a feature called AR spectrum with algorithm comparison. Using data in Figure 1, it predicts best results using the Data SVD FB algorithm over all others assuming two frequencies in the dataset (signal subspace = 4). Signal subspace is twice the number of spectral frequency components. One is for the real and one for the imaginary component. Optimal model order determination is an art at best. As model order increases, more of the data trends are incorporated into the model reducing uncertainty. If an order is selected which is greater than the optimum order, this adds noise which reduces uncertainty. AutoSignals order exploration feature predicts an optimum order between 40 and 50. This corresponds to two cycles in Figure 1. However, we still chose to explore errors as a function of model order before selecting an optimum order. We fit the spectrum over its full range with an adaptive n. We set added noise to its minimum value of 300 dB. This adds a fractional noise of 1E-15. AR results are listed in Table 1.

There are two types of errors listed in Table 1. Most algorithms report a frequency and frequency error. AR reports fit errors. These are rms errors between the data and the computed fit results. These are the exception in Table 1. Nonlinear optimization fits report frequency errors. Care must be exercised when comparing these results. Particularly with AR, a high fit error does not imply a high frequency error. In fact, we show that AR produces the best frequency error results but with poor fit errors.

All results, particularly fit errors, from any algorithm can be further refined using **nonlinear optimization (NLO)**. Autosignal uses an exponentially damped sinusoid model. Also, our nonresonant LITA waveforms have a time dependent baseline which we find can be approximated by a weakly damped sine wave. So, instead of using Equation 1, we use Equation 2 below.

$$Y(t) = A_1 * \sin(\omega_1 * t + \phi_1) * (\exp - B_1 * t) + A_2 * \sin(\omega_2 * t + \phi_2) * (\exp - B_2 * t) \quad (2)$$

It is a linear combination of two exponentially damped sinusoids. The first damped sinusoid models a low frequency oscillation which is a combination of the LITA baseline and the temporal profile of our probe laser. The second damped sinusoid models a high frequency oscillation representing the acoustic wavepackets. Both terms have independent phases and damping. Outputs from the AR method (DATA SVD FB, Order 50, SS=4) are used as initial guesses. LITA ordinate data typically spans ~1 order-of-magnitude. We expect linear-least-squares minimization to provide best results. Results in Table 1 confirm this and demonstrate no need for any of the three robust minimization approaches. We studied output with NLO as a function of order. We define optimal order as a compromise between minimal errors and minimal computation time. Hence, we select the lowest order possible. Table 1 shows optimal results using an order of 50. Since NLO should provide nearly optimum results, we conclude Figure 1 frequency is 20.169 MHz with 0.096% frequency error. This is used as the benchmark for comparison of frequency and error results between the different algorithms.

We distinguish between two types of results: those which come from a specific algorithm such as AutoRegressive and those which come from the nonlinear optimization routine. Virtually all algorithm results can be selected as input guesses to the NLO routine. If functioning properly, NLO results will converge to identical values independent of input guesses. However, different algorithms or improper order selection can provide poor guesses producing nonconvergence.

Optimal algorithms in Table 1 are not necessarily those with the lowest errors. Rather, it is those whose frequencies change least after nonlinear optimization and converge using a minimum number of iterations. Hence, they provide the best guesses to the optimization methods and are most likely to produce convergence. Within the AR method, Table 1 results indicate Data SVD FB is the optimal algorithm choice. This conclusion is supported by the math behind the method, discussions in the AutoSignal manual, and several trial fits with a few other algorithms (Burg, Autocorr, Nrml) using a few parameter variations (F, B, and FB) not included in Table 1. Using order = 50 and signal subspace = 4 (i.e. 2 frequency components), it computes 20.177 MHz with 5.26% fit error). Nonlinear optimization only refines this to 20.169 MHz with 3.06% fit error and 0.096% frequency error. There is a 0.0397% difference in the computed frequencies.

Autoregression computes a fit error but not a frequency error. The nonlinear optimization routine computes both. As shown above, both methods produce essentially identical frequency results. We conclude the error computed using nonlinear optimization can be assigned to the frequency computed using Autoregression with the DATA SVD FB algorithm with order 50 and signal subspace 4.

Fourier transforms are standard methods for undamped sinusoids. However, they have limited frequency resolution since computed frequencies are equally spaced and fixed in number. They are known to be inaccurate when applied to damped sinusoids. Table 1 results using five nearly equivalent Fourier algorithms show frequencies are 0.5-2.8% higher than NLO results with ~17x larger frequency errors.

Prony's method fits a linear combination of complex damped sines (AutoSignal approach) or complex damped exponential decays (ref. 1 approach) to uniformly sampled data. Damped algorithms are used since undamped methods are inappropriate for these waveforms. Results are presented as a function of order using SVD and NE algorithms. We were surprised that using SVD did not improve the frequency errors. SVD NE is designed for rapid computation of large datasets. It is known to produce results inferior to SVD and is very sensitive to noise. Fits are weakly sensitive to order (defined for Prony's as number of exponential decays fitted). Best results in Table 1 (Damped, order=30 SS=2) show frequencies (20.245 MHz) are ~ 0.38% higher than NLO results with 24x larger frequency errors. Since results are based on signal subspace of 2, they cannot be used as initial guesses for the NLO routine. Results from Prony's method used in reference 1 produce a frequency of 20.237 MHz and frequency error of 2.3%. These are nearly identical to Table 1 results.

Minimum Variance(MV) and EigenAnalysis(EA) methods are spectral estimators designed to discover harmonics in a waveform and graphically compare component powers. Their frequency resolution is typically slightly better than FFT's. Best MV results in Table 1 show frequencies within 0.17% of NLO results. However, most frequencies are ~0.6-0.8% higher than NLO results with 17x larger frequency errors. MV has no provision for order variation. NLO will not converge with these inputs.

EA results in Table 1 show frequencies nearly identical with NLO results. Music Fwd and EigVec Fwd have 16x larger frequency errors and wont converge. Music FB and EigVec FB have only 3x larger frequency errors and NLO converges. Higher orders may improve results. Autosignal EA routines are limited to order 100.

Based on Table 1 results, we conclude NLO using Equation 2 produces the most precise fit errors, frequency, and frequency errors (~0.1%). This requires initial guesses supplied by the AR spectral method using Data SVD FB algorithm with order = 50 and SS=4. If only frequency information is required, the AR method using Data SVD FB algorithm provides results nearly equivalent to the NLO results but with minimal computations and no initial guess requirement. NLO requires ~ 0.1 sec using a 3.2 GHz Pentium 4. EA is also viable but with increased frequency uncertainty(~0.3%). All other algorithms including Prony's produce inferior results(~1.5-3% frequency errors).

3.3 Mathematics of Selected Algorithms

3.3.1 Prony's Method Spectral Analysis Algorithms

The waveform to be analyzed is Y(t) and consists of N evenly spaced samples. For analysis using Prony's method, it can be expressed either as the sum of complex conjugate and real exponentials

$$Y(t)= \sum_{j=1}^{m} a(j) * \exp(-i\omega(j)t + \Phi(j)) * \exp(-k(j)t) \quad (3a)$$

or as the sum of exponentially damped sinusoids

$$Y(t)= \sum_{j=1}^{m} a(j) * \exp(-k(j)t) * \cos(\omega(j)t + \Phi(j)) \quad (3b)$$

Here, m is the order and refers to the number of equations which will be summed to describe the waveform. For a given equation, a(j) is the amplitude, k(j) is the damping coefficient, ω(j) is the frequency in hertz, and ϕ(j) is the phase in radians. Prony's method computes the complex parameters of each equation and then provides the four real parameters(a(j), k(j), ω(j), and ϕ(j)) for each equation.

We fit Y(t) data in Reference 1 to Equation 3a and use m= 40. AutoSignal uses Equation 3b. AutoSignal fits in Table 1 are based on one frequency component (signal subspace of 2). Both approaches produce equivalent results.

3.3.2 AutoRegressive Spectral Analysis Algorithm

The AR model is defined as follows

$$Y(k)= \sum_{j=1}^{p} a(j) * x(k+j) \quad , \; k = p \ldots 1 \qquad (4)$$

$$Y(k)= \sum_{j=1}^{p} a(j) * x(k-j) \quad , \; k = p+1, \ldots N$$

Where x is a data series of length N and a is AutoRegressive parameter array of order p. AutoSignal uses a positive sign convention(linear prediction) for the AR coefficients. This model is defined as backward prediction for the first p values and forward prediction for the remaining N-p values.

3.4 Comparison Between Autoregressive (AR), Autoregressive with Non Linear Optimization (AR+NLO), and Prony's methods

3.4.1 Single Waveform Results

Using data in Figure 1, we examine both graphically and numerically the results from AR, AR with NLO, and Prony's method. We begin by comparing power spectra results between AR and Prony's method. Results for 303K data in Figure 1 are shown in Figure 3. AR produces both a sharper frequency distribution and better S/N (i.e. 45 dB versus at best 30 dB) for Prony's. Clearly, AR can generate a more precise frequency and frequency error.

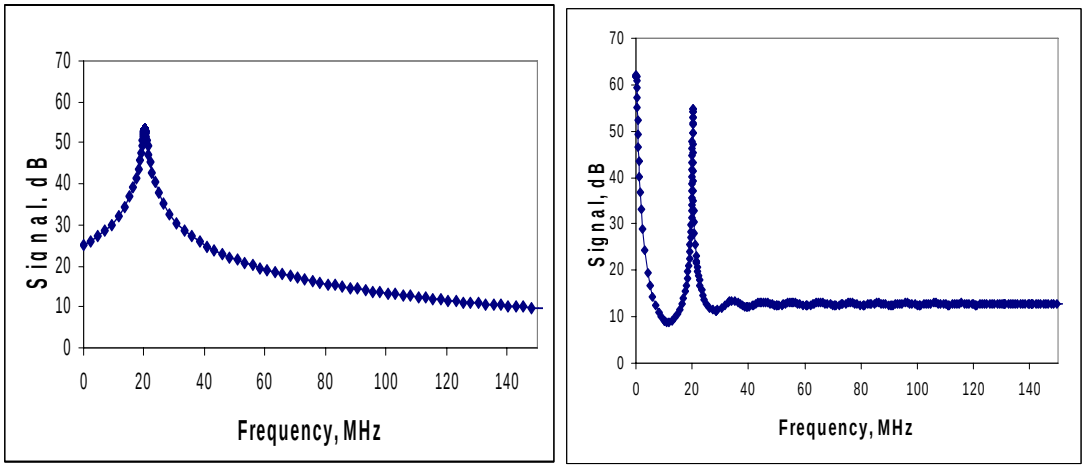

Figure 3. Power spectrum in dB using Prony's method (left) (Damped, order=30, SS=2) and AutoRegressive method (right) (Data SVD FB order=50 SS=4) for 303K data in Figure 1.

The results of the AR method provide more accurate inputs for the NLO routine. AR with NLO computed waveforms using Equation 2 are shown (Figure 4A). These are summed and overlaid with Figure 1 data (Figure 4B). Fit results using AR, AR with NLO, and Prony's method are given in Table 2. Component 1 is defined as the low frequency baseline. Component

2 is defined as the high frequency acoustic wavepackets. Visually, the frequency accurately matches the data throughout the entire waveform. This is in contrast to Figure 3 in Reference 1 using Prony's method. It appears to accurately match the frequency early in the waveform but predicts a slightly higher frequency with increasing time for both the 292 and 652K data. Results in Table 2 using Prony's method produce a frequency (20.245 MHz) which is 0.38% higher than AR with NLO(20.169 MHz) and AR without NLO. Frequency errors comparing Prony's and AR with NLO in Table 1 differ by a factor of ~18.

Comparing AR with AR with NLO, Table 2 shows nearly identical frequencies, phases, and powers. However, AR results for amplitude are inferior to those of NLO. This produces larger AR fit errors. We conclude AR with NLO produce the optimal fit results. If only frequency information is required, we recommend the AR method. Since no NLO processing is required, it is computationally faster. It requires no initial guesses and produces equivalent frequency results. We note that the AR spectrum is produced by modeling the waveform. Hence it is not artificially constrained as is Equation 2. Therefore, one could argue that it may produce frequency results which are more accurate than the NLO routine.

Our current LITA apparatus has insufficient accuracy to experimentally validate these numerical results. Since both AR and AR with NLO use different math methods to compute their results, this provides confidence in the frequencies and their associated errors. Using this fact, Prony's method frequencies and errors, and the Prony's graphical fits in reference 1, we conclude Prony's method is producing the poorest fit results.

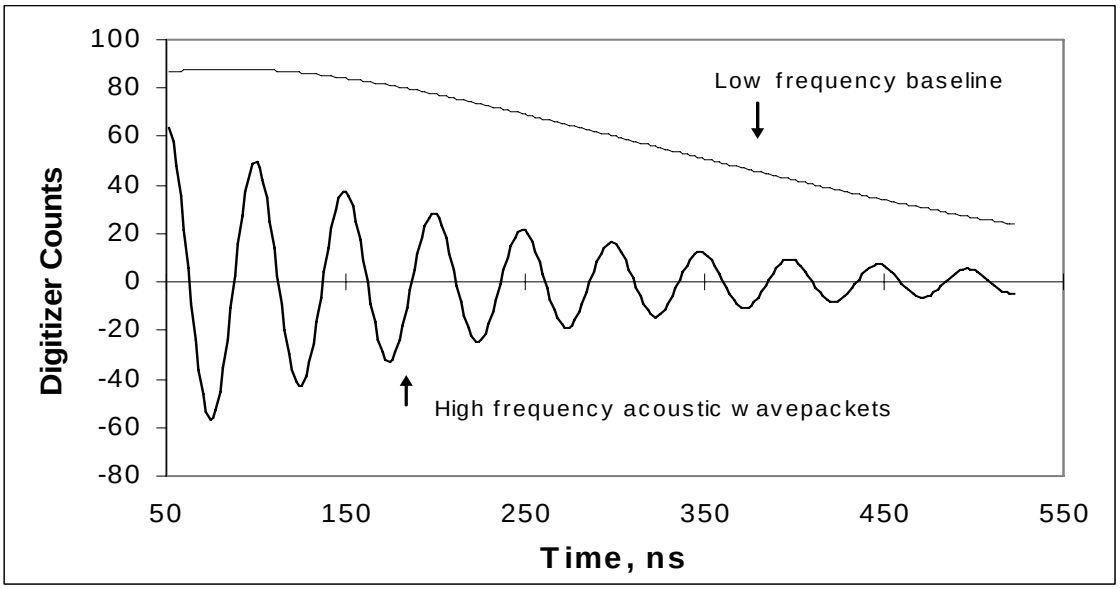

Figure 4A. Autoregressive method with nonlinear optimization (AR with NLO) computed waveform components from Equation 2 in Table 2 which are summed to produce bottom figure fit.

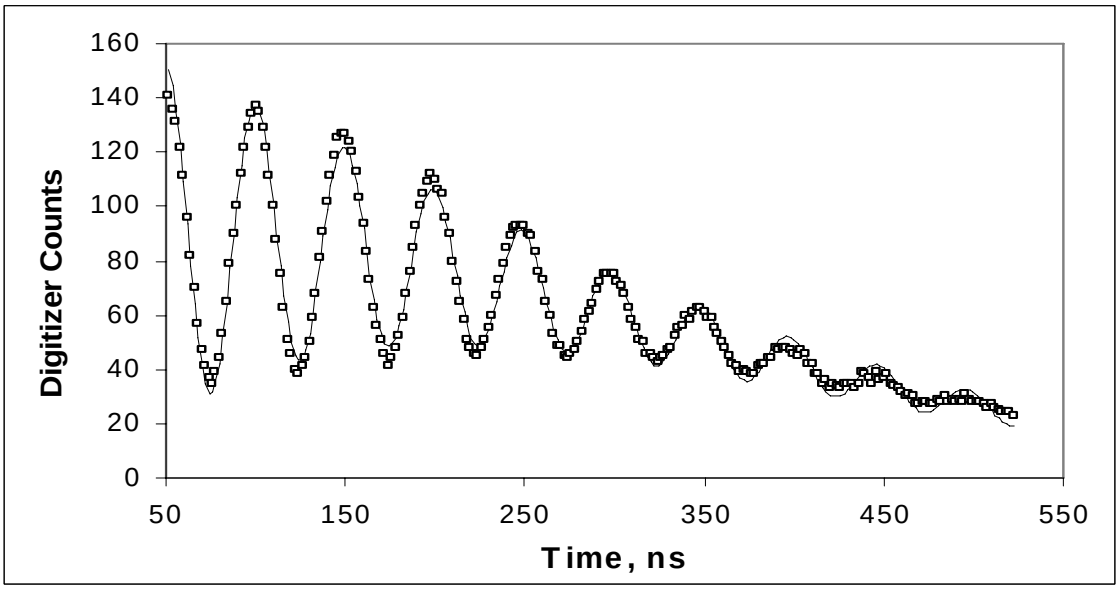

Figure 4B. Experimental LITA data (squares) and overlaid AR with NLO computed fit (line) using 303K data from Figure 1. Correlation coefficient (r^2) =0.9895.

Table 2. Comparison Between AutoRegressive (AR), AutoRegressive with Non Linear Optimization (AR+NLO) Fit Parameters (Equation 2), and Prony's Methods Numerical Results using Waveform in Figure 1 at 303K. AR + NLO Results are Used to Generate Waveforms in Figure 4B.

Method	Sinusoid	Amplitude	Freq, MHz	Phase	Damping MHz	% Power	Fit Error
AR+NLO	Component 1	205	0.479	0.387	3.97	91.3	
	Component 2	86	20.169	0.46	5.54	8.7	
							3.06%
AR	Component 1	109	0.277	2.04	----	94.4	
	Component 2	22	20.177	1.43	----	5.6	
							5.26%
Prony	Component 1	64	20.245	1.46	4.91	100.	----

3.4.2 Results Using 100 Waveforms

To insure results in Tables 1 and 2 are not limited only to Figure 1 data, we analyzed 100 waveforms from reference 1 using AR, AR with NLO, and Prony's methods at both 303K and 652K. Single shot results of frequency, frequency error and their associated histograms are presented in Figures 5-7. Figure 1 data is the first shot in this series. Average results and uncertainties are presented in Table 3.

In Figure 5, frequencies at 303K as a function of laser shot tend to be symmetrically distributed about 20.3 MHz. Figure 5 histogram shows shots are tightly grouped within ±0.3% (57 shots at 20.30 ±0.06 MHz). Figure 6 histogram shows errors are tightly grouped (83 shots between 0.08% and 0.10% error). There are 17 shots with errors > 0.1%. We inspected individual shots but could find no correlation between frequency and frequency error.

Frequencies and frequency errors using Prony's method are shown in Figure 7 and Table 3. Average frequency is 20.366 MHz with 1.76% error.

Using all data in Figures 5 and 7, we computed an unweighted mean and standard deviation. A similar analysis was performed with the frequency errors in Figure 6 and Figure 7. Results are shown in Table 3 for 303 and 652K data. Prony's frequencies are centered near 20.366 MHz with average error of 1.76% while AR with NLO frequencies are centered at 20.305 MHz with 0.095% error. These algorithms produce average frequencies which differ by ~0.4% and average frequency errors which differ by a factor of ~18. These results are similar to those above for the single waveform. They confirm our conclusions and demonstrate that the AR method is more precise when computing the frequency and frequency error over this ensemble of spectra than Prony's method. However, the unweighted standard deviation of the mean of 100 frequencies produced using AR analysis did not improve relative to Prony's method. We attribute this to pulse-to-pulse frequency fluctuations in our apparatus.

Frequency fluctuations can arise from temperature fluctuations in the oven and fluctuations in the LITA apparatus. Results in Figure 5 are uniformly distributed about 20.3 MHz as a function of time. This suggests oven temperature was essentially constant during the 10 seconds required to acquire 100 shots. This is supported by the following facts. We used a sealed cell isolated from room air currents. Cell is surrounded by oven weighing 165 lbs (i.e. a large thermal mass). For data at 303K, no power was applied to oven. The result is a slow cool down to room temperature and a presumed constant temperature during a 10 second data

acquisition time. We conclude the main contribution to frequency fluctuations in Figure 5 are fluctuations in the LITA part of our apparatus.

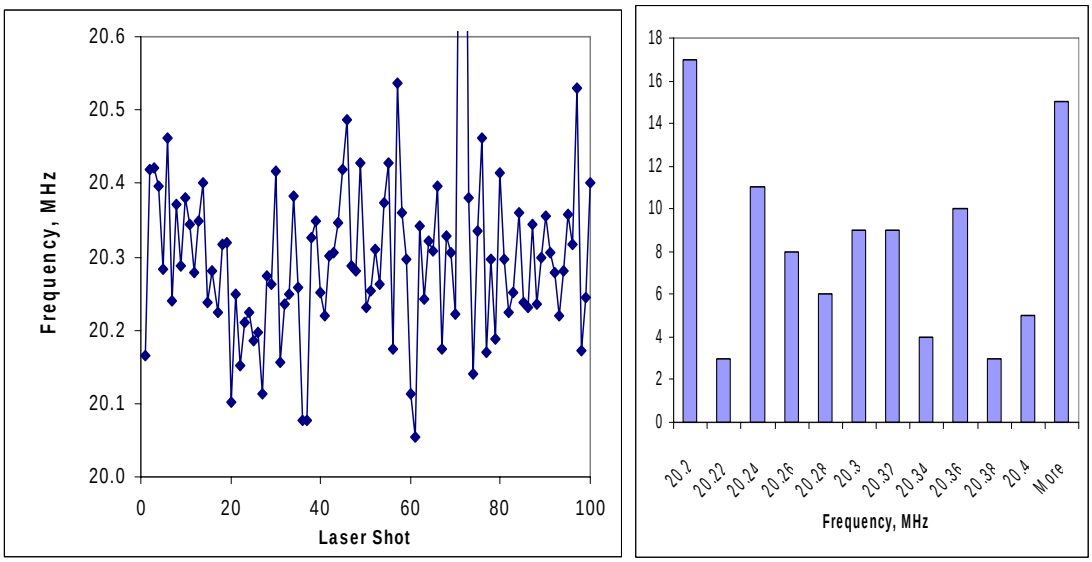

Figure 5. Autoregressive method with nonlinear optimization (AR with NLO) computed frequencies (left) and histogram (right) using 303K data for 100 laser shots. 57 shots are at 20.30 ± 0.06 MHz.

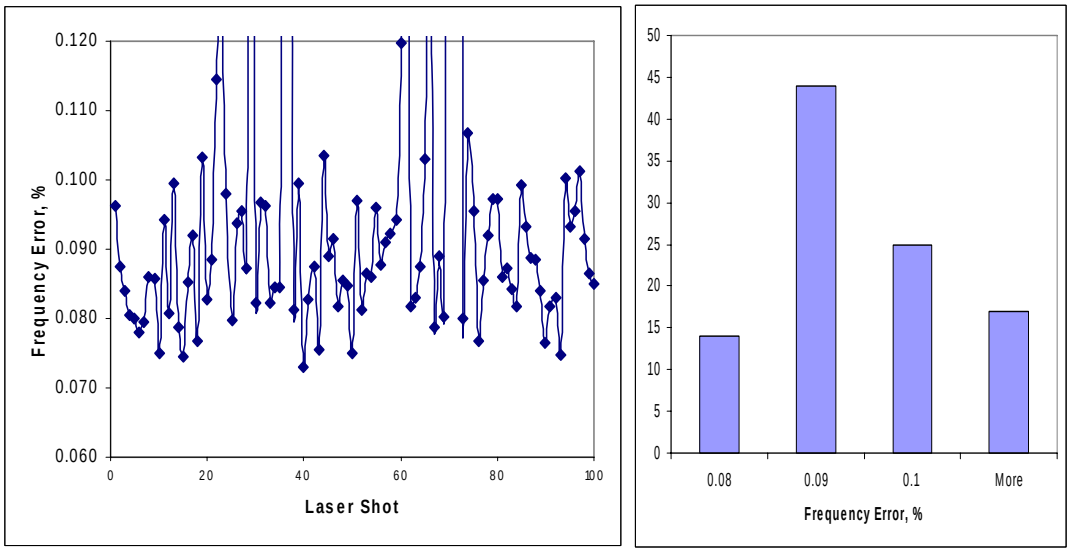

Figure 6. Autoregressive method with nonlinear optimization (AR with NLO) computed frequency errors in % (left) and histogram (right) using 303K data for 100 laser shots. 83 shots have between 0.08 and 0.10% error.

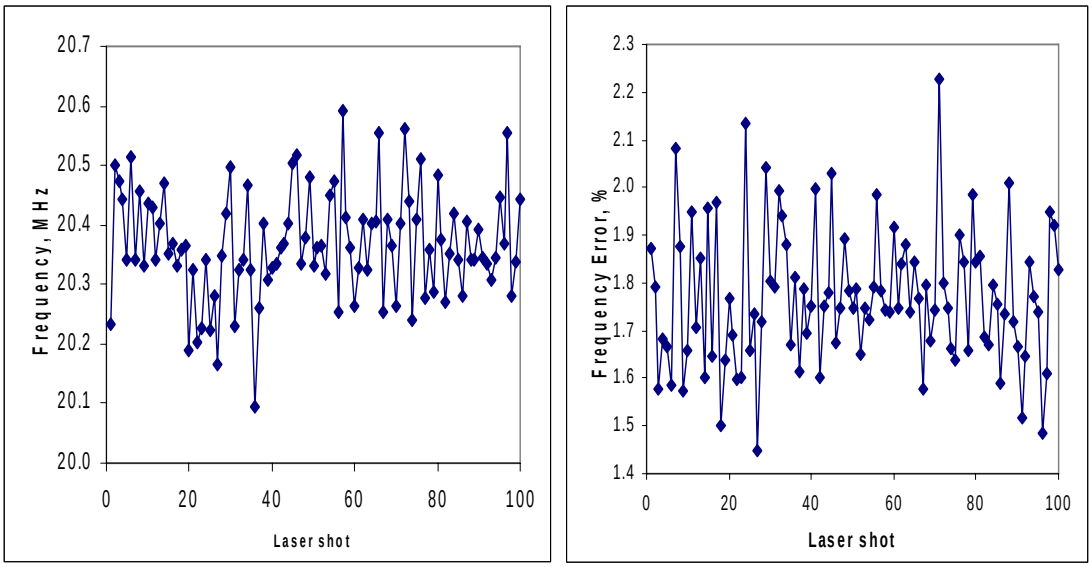

Figure 7. Prony's method computed frequencies(left) and frequency errors (%, right) using 303K data for 100 laser shots. (Damped, order=30, SS=2)

We also computed the average fit frequency and frequency error using a weighted average. Results are shown in Table 3 for 303 and 652K. Weighting reduces the frequency uncertainty of both methods by an order of magnitude. Essentially, this is a simple method to discard outlier results. By comparison, results in Reference 1 used residuals, noise, along with power spectral peak width and area as criteria to reject outliers. Typically 90 shots passed. Here, based on the histogram in Figure 6, 17 shots with errors above 0.1% are weakly weighted. Still, with AR's higher precision, 83 shots contribute to the weighed average. AR with NLO results indicate an average weighted frequency error of 0.009%.

To further study differences in the frequencies obtained using these algorithms, we calculated for 100 shots on a shot by shot basis, individual percent frequency differences between Prony's and AR with NLO (i.e. (P-NLO)/NLO *100) and frequency differences between AR with NLO and AR without NLO (i.e. (AR-NLO)/NLO *100). Results and histograms are given in Figures 8 and 9. On a shot by shot basis, Prony's frequencies are 0.3-0.6% higher versus AR with NLO while AR without NLO are < 0.10% of the AR with NLO results.

The results of this study indicate thermometry results in Reference 1 suffer minor errors due to Prony's method inadequacies. However, errors are well within the stated uncertainties of that work. Also, results are based on sound-speed ratios referenced to room temperature results. This tends of minimize small frequency errors.

Table 3. Frequencies (mean ± 1σ) and Frequency Errors (% error of fits), (mean ± 1σ) Associated with Weighted and Unweighted Analysis of 100 LITA Waveforms using AR with NLO and Prony Methods.

	AR with NLO		Prony		% Error Improvement Factor
Unweighted					
T(K)	Freq, MHz	% Error	Freq, MHz	% Error	
303	20.305 ± 0.15	0.095 ± 0.027	20.366 ± 0.091	1.76 ± 0.14	19x
652	30.43 ± 0.17	0.178 ± 0.042	30.539 ± 0.169	3.15 ± 0.56	18x
Weighted					
T(K)	Freq, MHz	% Error	Freq, MHz	% Error	
303	20.29720 ± 0.00183	0.0090	20.364 ± 0.036	0.177	20x
652	30.4381 ± 0.0051	0.0168	30.5396 ± 0.093	0.305	18x

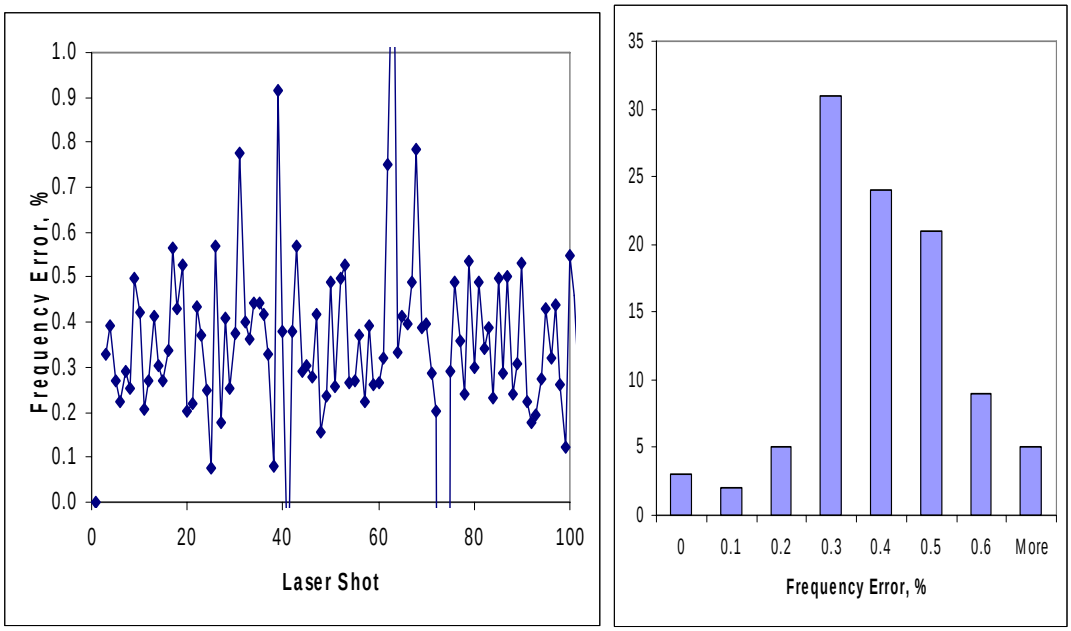

Figure 8. Data analysis comparison between Prony's method(P) and Autoregressive with nonlinear optimization (NLO) i.e. (P-NLO)/NLO *100 using computed frequencies(left) and histogram(right) for 303K data for 100 laser shots.

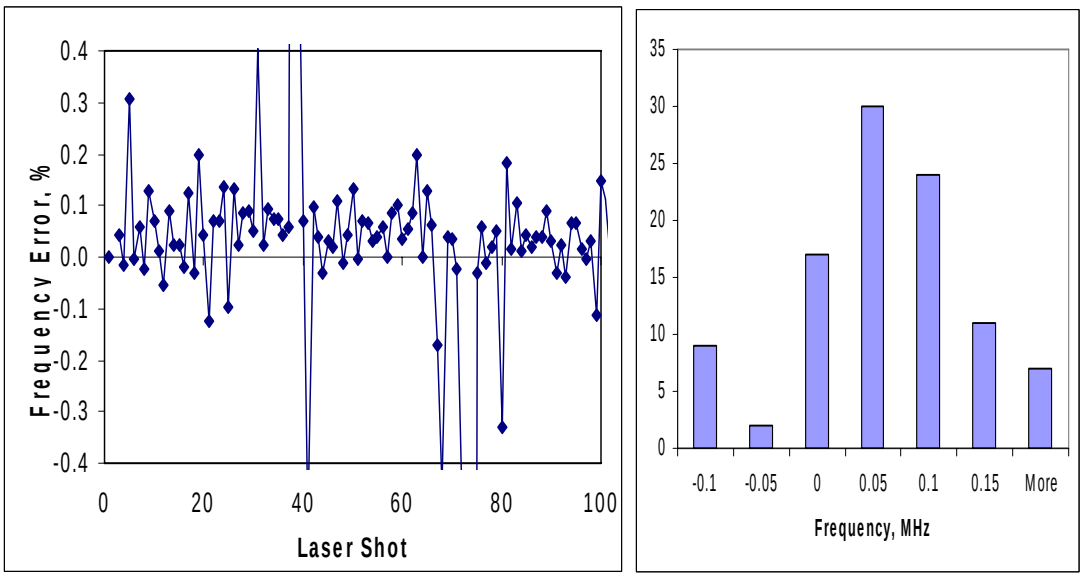

Figure 9. Data analysis comparison between AutoRegressive(AR) method and AutoRegressive method with nonlinear optimization(AR with NLO). (AR-NLO)/NLO*100 using computed frequencies(left) and histogram(right) for 303K data for 100 laser shots.

3.4.3 Discussion

There are several reasons why AR produces frequency and frequency error results superior to Prony's method.

First, the AR spectrum is produced by modeling as opposed to other methods such as Prony's which are transforms. It is a linear non-iterative matrix method. The DATA and FB options process the full forward and backward prediction data matrix to produce high accuracy results. It is known to have less bias in frequency estimate of spectral components and reduced variance in frequency variance over an ensemble of spectra(6). It is particularly well suited for the limited number of data points typical of LITA waveforms. Adding the SVD method forces robust predictions which are based on signal components, minimally influenced by noise, and exceedingly sharp. The adaptive n option uses a Runge-Kutta procedure to integrate the spectrum adaptively. This produces a frequency set concentrated near the peaks and an accurate area under the spectrum.

Second, AR results are further refined albeit modestly using nonlinear least-squares optimization with a standard Levenberg-Marquardt routine using Equation 2. Fit errors are reduced by a factor of 2 while frequencies changes by < 0.1%. Although not derived rigorously as Equation 1, Equation 2 describes the nonresonant LITA waveform produced by our experimental apparatus. It is limited to two frequency components and is an 8 parameter fit. Prony's requires 40 equations. This results in less interaction between fit parameters and more certain results.

At first glance, these exceptional results seem unjustified since Equation 2 has a different functional form compared to Equation 1. As discussed in section 3.2, the first damped sinusoid well describes the combined temporal profiles of our probe laser and LITA baseline. Our probe laser is a pulse stretched Alexandrite whose temporal profile compares well with computed baseline waveform in figure 4A. By comparison with equation 1, the second damped sinusoid in equation 2 should be squared. However, in nonresonant LITA, pulse-to-pulse spatial nonuniformities in the pump laser create nonuniform intensities in the counterpropagating acoustic wavepackets. Therefore, neither equation 1 nor the second sinusoid in equation 2 are the true functional form. The true function is between these extremes and pulse dependent. Hence, we consider the use of a damped sinusoid to be a reasonable approximation. Combined, these two effects are reasonably well described as the sum of two damped sinusoids. We conclude Equation 2 is justified.

The increased frequency resolution possible using the AR method has revealed a curiosity in this LITA data. Two frequency component fit residuals show a clear oscillatory behavior. This generally indicates another frequency component exists in the data. To test this we refit the data using 3 components (i.e. signal subspace 6). The fits are in a word perfect with r2 = 0.999. Data in Figure 1 at 303K produces 19.090 MHz (±0.50%) and 20.728 MHz (± 0.29%). Amplitude, phase, damping, and power are similar for both frequencies. However, we see no physical reason for the existence of a third frequency. Currently, we consider it an artifact of the model, the fitting routine, our LITA apparatus, or the low data sampling rate. However, we observe nearly symmetrical frequency splitting and similar characteristics of amplitude, phase, damping and power. One possibility is that we are seeing the beat frequency between the low-frequency oscillation (0.479 MHz) due to the combined baseline and probe laser profile and the high frequency oscillation due to the acoustic wavepackets(20.169 MHz). This would produce 20.169 – 0.479 = 19.69 MHz and 20.169 + 0.479 = 20.648 MHz i.e. nearly our observations. A more remote possibility is that we are somehow detecting frequency differences in the counter propagating acoustic wavepackets. It is hoped an improved LITA apparatus with a higher sampling rate (discussed below) will shed some light on this curiosity. No evidence for a fourth frequency component was detected.

3.5 Sample Rate Study

The AR power spectral density function is defined as follows[7]

$$P_{ar}(\omega) = \frac{\sigma^2 \Delta t}{\{1+ \sum_{j=1}^{p} a(j) * \exp(-i\omega k\Delta t)\}^2} \qquad (5)$$

Here, σ is the white noise variance and Δ t is the sampling interval. This equation shows that fit uncertainty improves as sampling interval decreases. Although derived for the Autoregessive method, the general concept is applicable to all methods. Hence we undertook a sampling rate study to understand how this can further improve fit precision and accuracy.

Table 4 provides data on frequency error improvement with increased sampling rate using the AR analysis method with nonlinear optimization. For this study, we require a highly-stable highly-accurate frequency source. We choose a function generator which produced a 100 mV undamped sine wave at 20.000 000 MHz with ±5 ppm stability(0.0005% frequency error). We acquired 500 ns of data at sampling rates of 0.1, 0.5, 2.5, and 20 GHz using a digital oscilloscope (2.5 GHz analog bandwidth, 40 GHz sampling rate). Results in Table 4 show that as sample rate is increased by a factor of N, frequency error is reduced by $\sqrt{N}$. This is essentially Felgett's advantage. However, it was achieved with sampling rates well above the analog bandwidth of the oscilloscope.

Results in Table 4 at 20 GHz show frequency error (0.0016%) is only a factor of ~3 greater than the manufacturer's instrument uncertainty(0.0005%). Hence, the AutoRegressive method is capable of this level of accuracy. Note that LITA result errors, albeit for damped sinusoids, are nearly two orders-of-magnitude larger. This study provides confidence in the precision and accuracy of the fit errors computed for damped sinusoids.

Table 4. Sample Rate Study using AutoRegressive Method (Data SVD FB, Order 40, Signal Subspace 2) with Non-Linear Optimization.

Sample Rate, GHz	Data Points	Computed Frequency, MHz	Frequency % Error	Improvement Factors √N Theory	Measured
0.1	50	20.000	0.0191	------	------
0.5	250	19.997	0.0088	2.2	2.2
2.5	1250	19.999	0.0043	5.0	4.4
20.0	10000	20.000	0.0016	14.	12.

3.6 Cycle Reduction Study

We are interested in applying LITA to supersonic and hypersonic wind tunnels along with combustors. These are low-density applications where acoustic damping is large. The result is a limited number of cycles and larger fit and frequency errors. Hence we studied errors as a function of number of cycles for damped and undamped sinusoids. We used AR with NLO and Prony's method to quantify errors.

3.6.1 Damped Sinusoid

Results of a cycle reduction study comparing AutoRegressive method with nonlinear optimization to Prony's method using Figure 1 data at 303K are shown in Table 5. For AR with NLO, they show 0.14% frequency errors with 2 cycles. Data from 1.5 cycles produced a frequency but NLO results would not converge. By comparison, Prony's method produces comparable frequency results but with errors which increase from 2% with 9 cycles to 12% with 1.5 cycles. Prony's method errors are 20 times larger than AR with NLO over 9 cycles and 57 times larger than AR with NLO over 2 cycles. We conclude AR or AR with NLO is the superior approach for a limited number of cycles. We conclude by using AR or AR with NLO, LITA can be a viable diagnostic in low-density applications.

Table 5. Frequencies and Frequency Errors Computed as a Function of Cycles for Data in Figure 1 using AutoRegressive Method (DATA SVD FB, SS=4) with Nonlinear Optimization and Prony's method.

	AR with NLO			Prony's	
	Freq,	Freq.		Freq,	Freq,
Cycles	MHz	% Error	Order	MHz	% Error
9	20.168	0.0983	50	20.303	2.05
8	20.170	0.101	50	20.305	2.27
7	20.144	0.109	50	20.303	2.55
6	20.187	0.106	80	20.292	2.94
5	20.179	0.116	80	20.308	3.46
4	20.300	0.142	50	20.321	4.14
3	20.224	0.138	50	20.335	5.25
2	20.295	0.140	35	20.257	8.10
1.5	20.496	-----	---	20.403	12.0

3.6.2 Undamped Sinusoid

To further evaluate Table 5 results, we require knowledge of how accurately AR with NLO can extract the frequency and error of a known waveform as a function of number of cycles. To perform this study, data was simulated using the function generator described above to create a 20.000 000 MHz undamped sine wave with 200 mV peak value which fills the digitizer. Waveform was sampled using the digital oscilloscope described previously. Results are shown in Table 6 for 0.5 and 20 GHz sampling rates

For 10 cycles at 20 GHz, per cent frequency errors are only 3 times the stated function generator uncertainty. Errors for 9 cycle damped sine waves in Table 5 are 52 times higher. Although we are comparing damped and undamped sine waves, this study provides confidence in the computed frequencies and uncertainties produced using AR with NLO.

Using 0.5 GHz sampling, fits were stable with three cycles. For two cycles, results were unstable (i.e. they seldom converged). Data from one cycle would not converge. For 20 GHz sampling, fits were stable to two cycles. Minor instability was encountered with one cycle. Repeated attempts would occasionally produce convergence at 0.5 cycles albeit with higher uncertainties. Comparing 20 versus 0.5 GHz sampling rate for any specified cycle, we observe that % error follows a simple linear dependence. Within a given sampling rate, % error increases nonlinearly as number of cycles is reduced. Using an oversimplified model and plotting the inverse % error (1/y) versus number of cycles (x), we find at 0.5 GHz and 20 GHz respectively.

$$1/y = (-19.0 \pm 2.6) + (12.8 \pm 0.4)*x \quad (6)$$

$$1/y = (-49.3 \pm 6.2) + (52.4 \pm 2.8)*x \quad (7)$$

We conclude that using 20 GHz sampling, AR with NLO can determine frequencies with errors < 0.05% over 1-2 cycles for undamped sine waves.

Table 6. Frequencies and Frequency Errors as a Function of Cycles for 20 and 0.5 GHz Sampling of a 20.000 000 MHz Simple Undamped Sine Wave using AutoRegressive Spectrum (Data SVD FB, Order 50, Signal Subspace 2) with Non-linear Optimization.

	20 GHz sampling		0.5 GHz sampling	
Cycles	Freq, MHz	Error, %	Freq, MHz	Error, %
10	20.000	0.0016	19.997	0.009
9	20.000	0.0019	19.998	0.010
8	20.000	0.0023	19.999	0.012
7	20.000	0.0027	20.000	0.014
6	20.000	0.0034	19.996	0.019
5	20.001	0.0046	19.995	0.023
4	20.002	0.0065	19.997	0.035
3	19.999	0.0097	20.002	0.061
2	19.991	0.0179	19.987	0.093
1.5	20.000	0.0275	20.0	0.221
1	19.989	0.0502	--------	-------
0.5	20.3	0.110	--------	-------

3.7. Signal Reduction Study

LITA is a nonlinear optical method. Signal levels can vary significantly on a pulse to pulse basis. It is useful to study how errors vary as a function of signal level over the digitizer range for high sample rates. Unfortunately, our current LITA apparatus is not configured for 20 GHz sampling. We choose to study this effect using undamped sine waves created using the function generator described above. Results at five signal levels spanning 90% down to 4.5% of digitizer range are shown in Table 7. Errors are independent of signal level to approximately 18% of the digitizer range. Below this, they increase by a factor of 2.5 down to 4.5% of the digitizer range. By comparison, when damped sinusoid signals similar to those in Figure 1 dropped below 15% digitizer range, they often could not be fit with Prony's method. These results suggest AR with NLO is better than Prony's at fitting waveforms with low S/N.

Table 7. Signal Reduction Study using AutoRegressive Spectrum (Data SVD FB, Order 50, Signal Subspace 2) with Nonlinear Optimization of a 20.000 000 MHz Undamped Sine Wave using 10 cycles Sampled at 20 GHz.

Signal, mV	Freq, MHz	Error, %
200	20.000	0.0020
100	19.999	0.0015
40	19.999	0.0019
20	19.998	0.0028
10	19.999	0.0048

4. Conclusions

This study demonstrates that the AutoRegressive spectral analysis algorithm with nonlinear optimization(AR with NLO) produces optimal frequency results, frequency errors, and fit errors for analysis of nonresonant LITA waveforms with homodyne detection. The nonlinear optimization model is a linear combination of two damped sinusoids. Using 0.5 GHz sampling rate, this method provides 0.096% single laser pulse frequency error at 303K. This is a factor of ~20 improvement compared to previous results using Prony's method.

If only frequency information is required, this study recommends the AutoRegressive spectral analysis method using the Data SVD FB algorithm. For conditions of this study, results are optimized using a model order of 40 and signal subspace of 4. Frequencies are equivalent to those of the AR with NLO algorithm, require no initial guesses, and require less computation. Since the AR spectrum is produced by modeling, it should produce frequency results which are equivalent to the NLO routine. Since AR and AR with NLO compute equivalent frequency results and frequency errors using different mathematical approaches, they independently verify the computed frequencies and frequency precision.

Results are optimized for parameters specific to these datasets. If any parameter particularly sampling rate is altered, relevant sections of this study should be repeated to determine optimal fit conditions. Model order can be particularly sensitive to this effect.

This study demonstrates three advantages of higher sampling rates with undamped sinusoids. As sample rate is increased by a factor of N, frequency error is reduced by $\sqrt{N}$. Fits converge with low errors with a limited number of waveform cycles. Fits converge and errors are reduced with low signal levels. Similar results are expected for damped sinusoids. Therefore, this study recommends the highest possible sampling rate to reduce errors.

Results obtained by combining AR analysis with increased sampling rate suggest nonresonant LITA can be applied with high accuracy and precision in low-density environments such as combustors and hypersonic wind tunnels. Results suggest single shot errors < 1% are possible even when number of waveform cycles are limited to 2 cycles by acoustic damping.

This study suggests 0.001% or 1 part in 10^5 sound speed measurements are possible by combining the AR algorithm for data analysis (0.1% or better single shot frequency and frequency error precision), a high-sample-rate data acquisition system (10x error reduction using 50 GHz sampling), and waveform averaging (10x error reduction using 100 waveform average). Therefore, we advocate a long-term development effort with two goals. First, attempt to develop a high-stability high-sample-rate laboratory LITA instrument where most shots have 0.01% or better frequency accuracy and precision. Second, use existing methods(8) to build an oven with 1 mK temperature resolution and thermometer capable of verifying the 0.001% error level.

LITA measurements are the result of sound propagation in the free field. This is in contrast to standard methods such as resonators (spherical and cylindrical) and ultrasonic interferometers which are encumbered by boundaries. Uncertainties of the latter are typically 0.01% or less (9). Results of this study suggest that with additional development, LITA can rival these methods for fundamental acoustic measurements without the boundary issues.

5. References:

1. Hart, R. C., Balla, R. J., and Herring, G. C., "Non-resonant Referenced LITA Thermometry in Air", Applied Optics **38,** 577-584 (1999).

2. Hart, R. C., Balla, R. J., and Herring, G. C., "Optical Measurement of the Speed-of-sound in Air over the Temperature Range 300-650K", J. Acoust. Soc. Am. **108, 1**946-1948 (2000).

3. Hart, R. C., Balla, R. J., and Herring, G. C., "Simultaneous Velocimetry and Thermometry of Air by use of Nonresonant Heterodyned Laser-induced Thermal Acoustics", Applied Optics, **40,** 965-968 (2001).

4. Hart, R. C., Herring, G. C., and Balla, R. J, "Pressure measurement in supersonic air flow by differential absorptive laser-induced thermal acoustics", Optics Letters **32,** 1689-1691 (2007).

5. Cummings, E. B., "Laser-induced Thermal Acoustics: Simple Accurate Gas Measurements", Optics Letters **19,** 1361-1363 (1994).

6. Marple, L., "A new Autoregressive Spectrum Analysis Algorithm", IEEE transaction of acoustics, speech, and signal processing **ASSP-28(4),** 441-454 (1980).

7. Kay, S. M. and Marple, S. L., "Spectrum Analysis – A Modern Perspective ", Proc. IEEE, **69(11),** 1380-1419 (1981).

8. Moldover, M.R, Boyes, S. J., Meyer, C. W. and Goodwin, A. R. H., "Thermodynamic Temperatures of the Triple Points of Mercury and Gallium and in the Interval 217 K to 303 K". J. Res. Natl. Inst. Stand. Technol., **104,** 11-46 (1999).

9. Zuckerwar, A. J., *Handbook of the Speed of Sound in Real Gases*, Volume II, Measurements, (Academic Press, San Diego, CA. 2002) Chapter 8.

REPORT DOCUMENTATION PAGE

Form Approved
OMB No. 0704-0188

The public reporting burden for this collection of information is estimated to average 1 hour per response, including the time for reviewing instructions, searching existing data sources, gathering and maintaining the data needed, and completing and reviewing the collection of information. Send comments regarding this burden estimate or any other aspect of this collection of information, including suggestions for reducing this burden, to Department of Defense, Washington Headquarters Services, Directorate for Information Operations and Reports (0704-0188), 1215 Jefferson Davis Highway, Suite 1204, Arlington, VA 22202-4302. Respondents should be aware that notwithstanding any other provision of law, no person shall be subject to any penalty for failing to comply with a collection of information if it does not display a currently valid OMB control number.
PLEASE DO NOT RETURN YOUR FORM TO THE ABOVE ADDRESS.

1. REPORT DATE *(DD-MM-YYYY)*	2. REPORT TYPE	3. DATES COVERED *(From - To)*
01- 07 - 2008	Technical Memorandum	

4. TITLE AND SUBTITLE

Signal Analysis Algorithms for Optimized Fitting of Nonresonant Laser Induced Thermal Acoustics Damped Sinusoids

5a. CONTRACT NUMBER

5b. GRANT NUMBER

5c. PROGRAM ELEMENT NUMBER

6. AUTHOR(S)

Balla, R. Jeffrey; and Miller, Corey A.

5d. PROJECT NUMBER

5e. TASK NUMBER

5f. WORK UNIT NUMBER

599489.02.07.07.03.03.01

7. PERFORMING ORGANIZATION NAME(S) AND ADDRESS(ES)

NASA Langley Research Center
Hampton, VA 23681-2199

8. PERFORMING ORGANIZATION REPORT NUMBER

L-19491

9. SPONSORING/MONITORING AGENCY NAME(S) AND ADDRESS(ES)

National Aeronautics and Space Administration
Washington, DC 20546-0001

10. SPONSOR/MONITOR'S ACRONYM(S)

NASA

11. SPONSOR/MONITOR'S REPORT NUMBER(S)

NASA/TM-2008-215327

12. DISTRIBUTION/AVAILABILITY STATEMENT

Unclassified - Unlimited
Subject Category 64
Availability: NASA CASI (301) 621-0390

13. SUPPLEMENTARY NOTES

An electronic version can be found at http://ntrs.nasa.gov

14. ABSTRACT

This study seeks a numerical algorithm which optimizes frequency precision for the damped sinusoids generated by the nonresonant LITA technique. It compares computed frequencies, frequency errors, and fit errors obtained using five primary signal analysis methods. Using variations on different algorithms within each primary method, results from 73 fits are presented. Best results are obtained using an AutoRegressive method. Compared to previous results using Prony's method, single shot waveform frequencies are reduced ~0.4% and frequency errors are reduced by a factor of ~20 at 303K to ~ 0.1%. We explore the advantages of high waveform sample rates and potential for measurements in low density gases.

15. SUBJECT TERMS

Numerical methods; Ultrasonic acoustics; Laser induced thermal acoustics; Optics; Measurements

16. SECURITY CLASSIFICATION OF:			17. LIMITATION OF ABSTRACT	18. NUMBER OF PAGES	19a. NAME OF RESPONSIBLE PERSON
a. REPORT	b. ABSTRACT	c. THIS PAGE			STI Help Desk (email: help@sti.nasa.gov)
					19b. TELEPHONE NUMBER *(Include area code)*
U	U	U	UU	29	(301) 621-0390